Long-Term Temperature-Dependent Degradation of 175 W Chip-on-Board LED Modules

Herzog, Alexander; Wagner, Max; Benkner, Simon; Zandi, Babak; van Driel, Willem D.; Khanh, Tran Quoc

DOI
10.1109/TED.2022.3214169

Publication date
2022

Document Version
Final published version

Published in
IEEE Transactions on Electron Devices

Long-Term Temperature-Dependent Degradation of 175 W Chip-on-Board LED Modules

Alexander Herzog, Max Wagner, Simon Benkner, Babak Zandi, Willem D. van Driel, and Tran Quoc Khanh

***Abstract*— We report on the degradation dynamics and mechanisms of the commercially available chip-on-board (COB) high-power light-emitting diode (LED) modules with an electrical power of 175 W. Due to the associated thermal load, the temperature dependence of the aging processes is additionally analyzed within the scope of this work. The aging tests were performed for a period of 6000 h at four different case temperatures between 55 °C and 120 °C. The results of the accelerated stress tests indicate a temperature-activated aging process, which severely limits the lifetime of the modules. In addition, the following key findings can be reported: 1) a significant decrease in optical power occurs within 6000 h of operation; 2) depending on the stress test condition the accompanying color shifts exceed a limit of $\Delta u'v' = 0.007$; and 3) the limiting degradation mechanism can be attributed to the package of the device and can be accelerated with temperature, current, and chemicals. Reported findings can be manifested by additional optical material inspections, allowing to use the results for optimizations of future module generations.**

***Index Terms*— Accelerated aging, Ag mirror corrosion, chip-on-board (COB), color shift, high-power LED, LED modules, light-emitting diodes (LEDs), reliability.**

I. Introduction

In RECENT years, the light-emitting diode (LED) technology has become increasingly established in the field of general lighting due to its energy efficiency and compact design [1], [2]. Especially phosphor-converted white semiconductor light sources are of great importance in several lighting applications and have been continuously optimized and developed. By varying the phosphors applied to the blue LED chips, a wide range of polychromatic spectra can be realized, which can approximate almost any correlated color temperature (CCT) along the Planckian locus [3].

Due to the recent innovative manufacturing technologies, it has become possible to mount a large number of mid-power LED chips on a single carrier substrate [4]. By connecting the LED chips in series or in parallel, the chip-on-board (COB) modules with high power densities can be realized. The direct chip application on the carrier substrate allows to create low thermal resistances in the range of 0.08–0.15 KW^{-1}. In this way, it is possible to operate the modules with an electrical power of up to several hundreds of watts, if an adequate thermal interface is made to an appropriately dimensioned heat sink [5]. This technological development provides the fundamentals to design compact light sources, which can be used in spotlights for construction sites, warehouses, retail, and sport facilities. In addition, arbitrary polychromatic spectra can be mixed in a compact design space for the purpose of integrative lighting [6], [7].

The relevance of the thermal interface, however, becomes apparent due to the high electrical and the associated thermal load. Small changes in the thermal path, which could occur due to degradation effects, could have a significant impact on the junction temperatures, resulting in accelerated lumen depreciation of the modules [8]. The high power density of the module causes a steep temperature gradient within the device, resulting in high mechanical stress on the different components and layers of the LED module. Depending on the extent of the degradation mechanisms in particular device components, the lifetime of the entire LED module could be affected [9]. Therefore, the analysis of the aging mechanisms and their impact on lumen depreciation is useful, if the lifetime should be specified under different operating conditions.

The state-of-the-art investigations address the aging behavior of the high-power COB modules to a limited extent [10], [11]. Especially in the power class above 100 W, there are no empirical data published or analyzed regarding the aging behavior or the underlying degradation mechanisms of the COB modules.

To address the existing knowledge gap, we analyzed the temperature-dependent degradation dynamics of the 175 W COB modules within the scope of this study. The modules were operated at four different case temperatures and

Manuscript received 21 June 2022; revised 22 September 2022; accepted 6 October 2022. Date of publication 21 October 2022; date of current version 30 November 2022. This work was supported in part by the Electronic Components and Systems for European Leadership Joint Undertaking (ECSEL) Joint Undertaking (JU) through the European Union's Horizon 2020 Research and Innovation Program, The Netherlands, Hungary, France, Poland, Austria, Germany, Italy, and Switzerland, under Agreement 101007319; and in part by the German Government through the Federal Ministry for Economic Affairs and Energy under Grant ZF4080804LT6. The review of this article was arranged by Editor J. D. Phillips. *(Corresponding author: Alexander Herzog.)*

Alexander Herzog, Max Wagner, Simon Benkner, Babak Zandi, and Tran Quoc Khanh are with the Laboratory of Adaptive Lighting Systems and Visual Processing, Technical University of Darmstadt, 64289 Darmstadt, Germany (e-mail: herzog@lichttechnik.tu-darmstadt.de).

Willem D. van Driel is with the EEMCS Faculty, Delft University of Technology, 2628 CD Delft, The Netherlands, and also with Signify (former Philips Lighting), 5656 AE Eindhoven, The Netherlands.

Color versions of one or more figures in this article are available at https://doi.org/10.1109/TED.2022.3214169.

Digital Object Identifier 10.1109/TED.2022.3214169

constant current stress. Based on the results of the optical measurements, the changes in the spectral characteristics were analyzed for the aging period of 6000 h. The collected aging data allow conclusions to be drawn about the underlying degradation mechanisms, which can be used for the optimization of future product developments, regarding both the LED modules and their application constraints in luminaires.

II. Experimental Details

The experiments were carried out on the commercially available 175 W high-power COB modules with a CCT of 4500 K and a color rendering index of CRI = 80, produced by a leading manufacturer. The maximum forward current at a case temperature of $T_c = 25\,°C$ is specified with $I_{f,max} = 4200\,mA$, resulting in a luminous flux of 20 000 lm at an electrical power of $P_{el} = 175\,W$.

Typical characteristics of the analyzed samples at $I_f = 1000\,mA$ are listed in Table I.

The structure and the dimensions of the modules are shown in Fig. 1. Placing the electrical contact on the top of the semiconductor structures allows to mount 312 lateral mid-power LED chips directly on an aluminum carrier substrate. To increase the extraction efficiency of the device, the carrier substrate is deposited with a silver mirror layer. The substrate and the LED chips are coated with a phosphor layer, which is additionally encapsulated with silicone for an enhancement of light extraction.

To analyze the temperature-dependent degradation dynamics of the COB LEDs, the devices were mounted on heat sinks with forced cooling (Fischer LA10/150, LA7/150, and LA-HLV3-100). On each heat sink, four samples were operated under identical aging conditions. The setup is shown schematically in Fig. 2. The temperature of the COB LEDs is monitored using Pt-100 temperature sensors placed at the T_c-point of the modules, as shown in Figs. 1 and 2. An adjustment of the forced cooling fan speeds allows to set the different case temperatures. The thermal interface between the COBs and the heat sink was realized with thin graphite layers.

The aging was performed for a period of 6000 h at four different T_c temperatures and a constant current stress of $I_a = 3300\,mA$ (Meanwell HLG-185H 42A). In Table II, the experimental stress test conditions are reported. It is important to remark that the differently tempered heat sinks and devices were not operated in separate temperature chambers; instead, they were stored horizontally on a metal table in an air-conditioned laboratory. The ambient temperature of the samples can be quantified with $T_a = 25\,°C$ at a relative humidity of RH = 30%.

The junction temperatures shown in Table II were derived under consideration of the thermal resistances measured by a thermal impedance measuring system (T3ster, Mentor Graphics). For the analyzed samples, a thermal resistance of $R_{th} = 0.08\,KW^{-1}$ was determined on average. The selected aging conditions were both within and slightly above the maximum junction temperature ($T_{j,max} = 125\,°C$) specified by the manufacturer, allowing to accelerate the provoked degradation mechanisms by temperature.

During stress test, the measurement of the LEDs was performed in intervals of 1000 h using a 1 m-integrating sphere with 2π-geometry in combination with a spectroradiometer (CAS140CT, Instrument Systems). For each measurement, the LEDs were disassembled from the heat sinks and placed on an LED mount in front of the measurement port. The LED mount integrated Peltier element was controlled by a Peltier controller (ITC4020, Thorlabs) and was used to temper the LED during the pulsed measurement. Due to the minimum integration

TABLE I
Overview of Initial Device Characteristics at a Measurement Current of 1000 mA. The Reported Values Represent the Arithmetic Mean With Its Respective Standard Deviation

CCT (Kelvin)	Optical power (W)	Forward voltage (V)	Degradation time (hours)
4473 ±18	19, 11 ±0, 23	35, 70 ±0, 16	6000

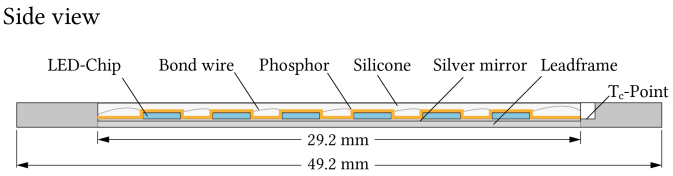

Fig. 1. Schematic cut view of the analyzed samples. Lateral mid-power LED chips are directly mounted on a silver-coated carrier substrate. The emitters are coated with phosphor and are encapsulated with silicone.

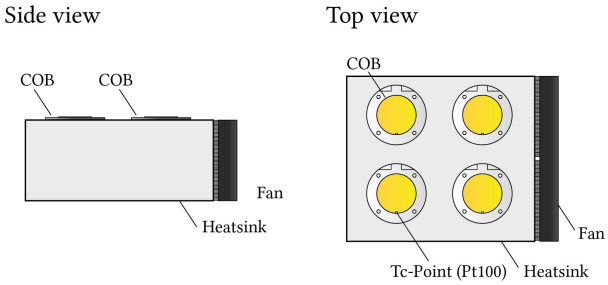

Fig. 2. Side and top views of the stress test setup. Four LED modules were mounted on each forced cooler. Case temperatures were monitored at the modules' T_c-points. The temperatures were adjusted by the forced coolers' fan speed.

TABLE II
Selected Test Conditions for the Performed Stress Test. Junction Temperatures are Calculated With Determined Thermal Resistance

Stress current I_a (mA)	Case temperature $T_c \pm 4\,K$ (°C)	Junction temperature $T_j \pm 4\,K$ (°C)
3300	55	61
3300	85	91
3300	105	111
3300	120	126

time of the spectroradiometer (10 ms), the synchronous current pulsewidth is set to 12 ms and limited to 1000 mA, reducing the effect of joule heating. An additional electrical characterization was performed using a source measure unit (Keithley 2651A). After performed measurement characterization, the modules were mounted on the heat sinks as before. To ensure a consistent thermal interface, the mounting screws were tightened with a torque wrench and the previously determined values.

III. Results

In Fig. 3 the decrease in optical power is shown for four different case temperatures at an aging current of $I_a = 3300$ mA. The measurements were carried out at $I_m = 1000$ mA. For a period of 6000 h, a reduction in optical power of 30% can be observed for a case temperature of $T_c = 120$ °C. As the case temperature decreases, the degradation rate in optical power decreases. At a temperature of $T_c = 55$ °C, a decrease in 5% can be measured.

Especially within the first 2000 h of operation, a significant decrease in optical power can be observed, the slope of which is reduced between 2000 and 6000 h. Since dropping below the L_{70} lifetime criterion is typically defined as a failure criterion for luminaires in the general lighting applications [12], lifetimes of more than 12 500 h can only be expected for junction temperatures below $T_j = 91$ °C, assuming a linear extrapolation of the aging data. Usually, lifetimes between 25 000 and 50 000 h are aspired in the LED-based luminaires, which can only be met by these devices at very moderate temperature conditions. To obtain more reliable statements regarding device lifetime, the aging tests must ideally be carried out with a higher number of samples and the lifetime should be calculated according to TM-21 [12].

Accompanying the gradual degradation of the optical power, an imbalanced reduction in spectral components can be observed, resulting in a color shift of the chromaticity coordinates. For a case temperature of $T_c = 105$ °C, the changes in the spectral characteristics are shown in Fig. 4. It becomes apparent that a significant decrease in power can be detected in the phosphor-converted region of the spectrum and in the blue spectral range.

For 6000 h of stress, a reduction of 8% can be measured at the peak emission wavelength at 450 nm, while the emission spectrum of the phosphor is reduced by 36%. The imbalance of the spectral changes results in a visually perceptible color shift. Fig. 4 (inset) shows the degradation of the blue and the phosphor-converted emission peak. It is clearly visible that the phosphor-converted part of the spectrum is subjected to much stronger degradation than the blue spectral components. In addition, the yellow-to-blue peak emission ratio is shown, indicating a significant color shift within the first 2000 h of operation. Analogous to the decrease in the optical power, the slope of the y/b ratio also reduces after this initial drop, resulting in a smaller but continuous color shift.

The color distance $\Delta u'v'$, which is defined as the Euclidean distance to the initial color coordinates [13], is shown for the entire stress test period in Fig. 5. Analogous to Fig. 3, the strongest degradation can be shown for the highest stress condition, resulting in a color shift of $\Delta u'v' = 0.022$ at a case temperature of $T_c = 120$ °C. The color shift is correspondingly smaller at lower device temperatures. If a commonly used color shift of the three-step MacAdam [14] or seven-step MacAdam [15] is defined as the degradation limit, this can only be maintained at a case temperature of 55 °C for the operating time considered.

Due to the missing directional information of the chromaticity shifts shown in Fig. 5, additional sections of the $u'v'$ diagram are presented in Fig. 6 [16]. For the different case temperatures, the one-, two-, and three-step MacAdam ellipses are shown to classify the color shift and its extent [17]. Based on the diagrams, it can be concluded that the direction of the blue shift does not differ between the temperatures. For the entire aging period, a CCT shift of $\Delta CCT = +1000$ K can be

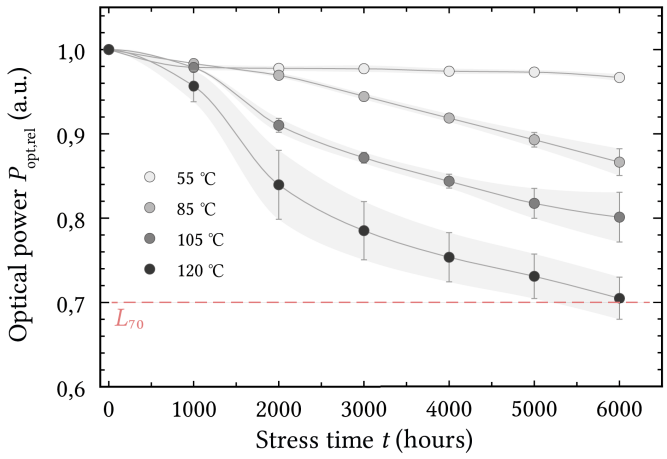

Fig. 3. Decrease in relative optical power $P_{opt,rel}$ for a period of 6000 h at four different case temperatures 55 °C, 85 °C, 105 °C, and 120 °C. The reported values represent the arithmetic mean with its respective standard deviation. A reduction of 30% in optical power, also known as L_{70} lifetime criterion, is shown as dashed.

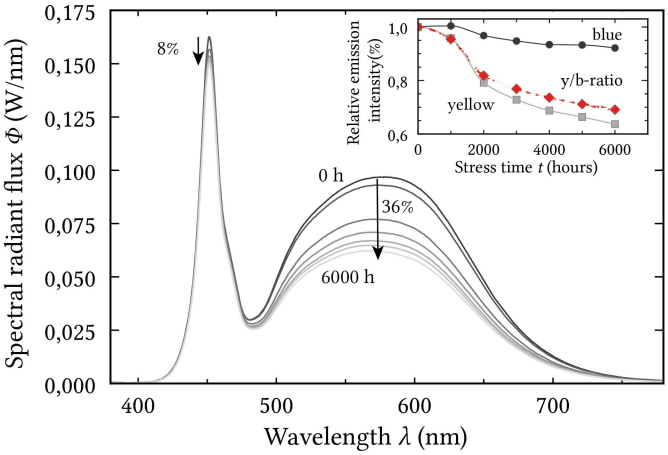

Fig. 4. Changes in spectral characteristics over 6000 h of stress test at a case temperature of $T_c = 105$ °C. Degradation of relative emission intensity at blue and yellow peaks of the spectrum (inset). The resulting y/b ratio is shown in red.

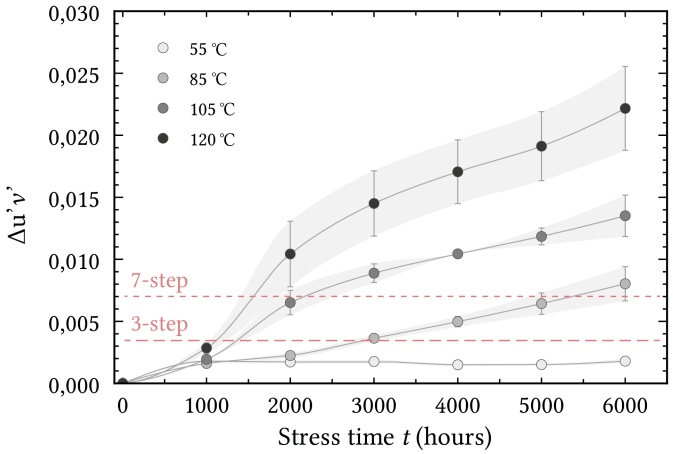

Fig. 5. Calculated color shift $\Delta u'v'$ at four different case temperatures. Shown are the mean values with the corresponding standard deviations. The three-step MacAdam $\Delta u'v' = 0.0033$ and the seven-step MacAdam $\Delta u'v' = 0.007$ failure criteria are shown as dashed.

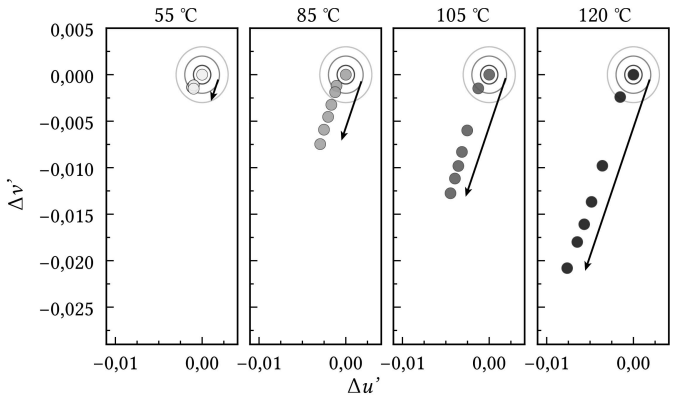

Fig. 6. Mean differences in color shift to the initial chromaticity coordinates shown in sections of a $\Delta u'\Delta v'$ diagram. The extend of the shift increases with temperature.

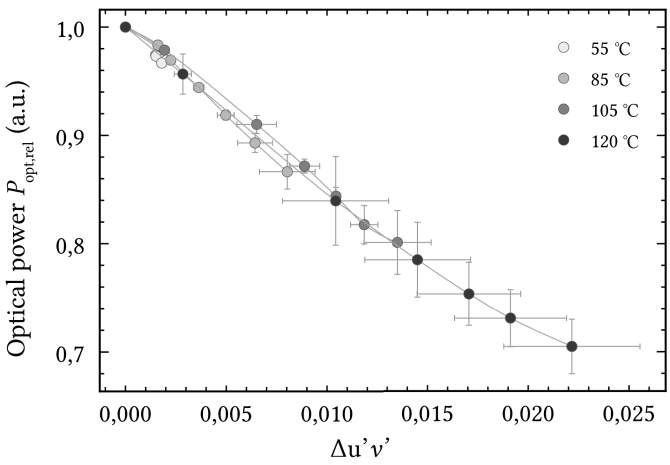

Fig. 7. Decrease in relative optical power $P_{opt,rel}$ versus calculated color shift $\Delta u'v'$ at four different case temperatures. Shown are the mean values with the corresponding standard deviations.

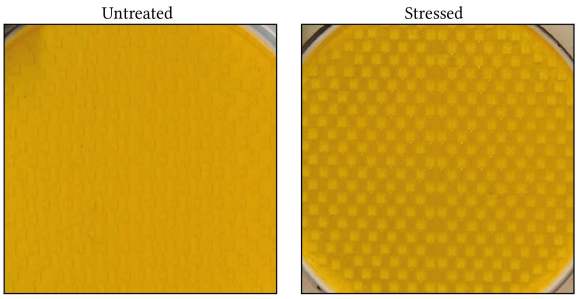

Fig. 8. Surface of untreated (left) and treated samples (right) at $T_c = 105$ °C after 6000 h of stress. The area between the LED chips is darkened as a result of degradation effects.

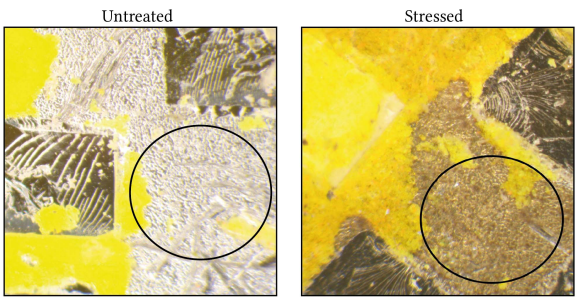

Fig. 9. Microscopic images of bared silver mirrors. Untreated and treated samples at $T_c = 105$ °C after 6000 h of stress. The LED chips were removed to inspect the area underneath.

observed for the highest temperature, while a shift of +80 K can be observed at 55 °C case temperature.

In addition to Figs. 3 and 5 the decrease in optical power versus chromaticity shift is plotted. The data shown in Fig. 7 indicate the different measurement times with the corresponding standard deviations. An almost linear correlation of the decrease in optical power and color shift could be obtained. At higher temperature, optical degradation, and consequently color shift, is more proceeded. The correlation is given for all the analyzed devices, respectively, and all the combinations of temperature, optical degradation, and color shift. Consequently, it would be possible to infer the optical degradation from the color shift and vice versa.

The visual inspection of the untreated and stressed modules is shown in Fig. 8. The direct comparison indicates a darkening of the silver-coated reflector in the area between the LED chips, which significantly reduces the reflection of the silver mirror. Areas below the LED chips are unaffected by the darkening process.

The microscopic images shown in Fig. 9 manifest the previously made assumptions regarding the darkening of the silver-plated reflector. The bared silver mirror shows a significant browning between the LED chips while the area below the removed LEDs is not affected.

To evaluate the temperature dependence of the aging mechanisms, a decrease in optical power by more than 12% is defined as a failure criterion L_{88}. The mean time to failure MTTF as a function of junction temperature results according to Fig. 10.

The logarithmic plot of the MTTF versus the inverse junction temperature indicates a temperature-accelerated aging process which can be described with a coefficient of determination of $R = 0.99$ using an Arrhenius equation. Applying

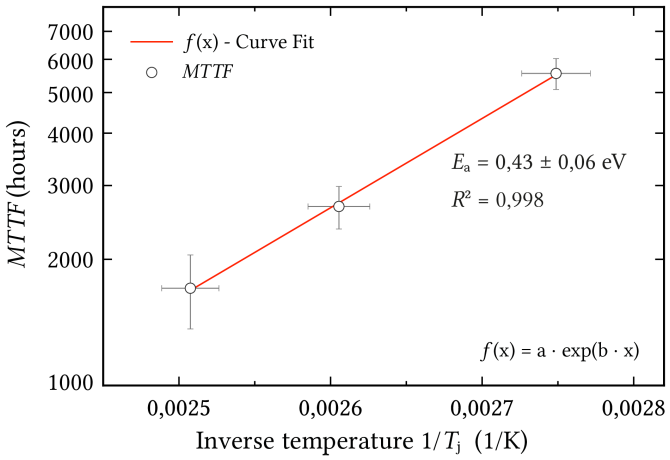

Fig. 10. Arrhenius plot of the 88% MTTF. The criterion has been chosen to analyze the data of three different temperatures without additional extrapolations. Based on the 88% lifetimes, an activation energy of $E_a = 0.43$ eV could be determined for the aging process with a coefficient of determination of $R = 0.99$.

the curve fit shown in Fig. 10, the activation energy of the process can be determined, resulting in $E_a = 0.43$ eV and thus suggesting a strong temperature dependence of the degradation process.

IV. Discussion

The strong temperature dependence of the degradation dynamics suggests that the package is significantly involved in the aging processes. In particular, the degradation behavior described above can result from the mechanisms in the phosphor, the silicone encapsulant, or the silver mirror used [18], [19], [20], [21]. The combination of intense short-wave radiation and high package temperatures (>100 °C) favors the aging mechanisms in the silicone encapsulation of the device [21]. Due to the fact that a reduced transmittance of the encapsulant predominantly affects the shortwave radiation components, a red shift of the spectral characteristics would be expected [18]. On the basis of the analyzed aging data, this mechanism cannot be manifested, especially since a blue shift of the spectrum can be observed. Therefore, the optical power reduction could be caused by the following mechanisms.

1) A loss of phosphor quantum efficiency due to chemical change or temperature effects.
2) Oxidation of the molding compound in plastic leaded chip carrier (PLCC) or "tarnishing" of exposed metal surfaces.
3) Operating the phosphor above the saturation flux level, settling, and precipitation of the phosphor.
4) Top-to-bottom fractures of the binder in the phosphor-binder layer, resulting in blue photons bypassing the phosphor layer [22].

As a result of the design and structure of the modules, the settlement effects of the phosphor can be ruled out. Fractures of the binder cannot be detected on the basis of optical inspections. Instead, a change in the reflective properties of the silver reflector can be manifested. Although silver coatings are predestined for optical applications due to their optimal reflective properties, unprotected silver coatings tend to oxidize [23]. The oxidation process, also known as "tarnishing" of the silver, results in the formation of a black patina, which protects the underlying silver layers from further oxidation processes. As the silver tarnishes, the reflective behavior changes, especially in the blue and green spectral range, causing short-wave radiation to be absorbed more strongly [24]. The oxidation reaction can be accelerated by sulfur, halogens, chlorines, iodines, or bromides in the region of the silver reflector [25], [26].

The permeability of the silicone encapsulant allows chemicals to diffuse into the region of the silver reflector. In combination with oxygen, temperature, and radiation prevailing in the device structure, a diffusion of sulfur, halogens, and volatile organic compounds (VOCs) could cause an oxidation of the used silver mirror. Typical reactions resulting in a tarnished silver are listed below [25], [27]

$$4\mathrm{Ag} + \mathrm{O_2} \longrightarrow 2\mathrm{Ag_2O} \quad (1)$$

$$4\mathrm{Ag} + 2\mathrm{H_2S} + \mathrm{O_2} \longrightarrow 2\mathrm{Ag_2S} + 2\mathrm{H_2O} \quad (2)$$

$$2\mathrm{Ag} + \mathrm{S} \longrightarrow 2\mathrm{Ag_2S}. \quad (3)$$

The formation of the black silver patina reduces the percentage of blue radiation reflected by the silver mirror. Due to the longer path length of the radiation from the chip via the reflector through silicone, it can be assumed that radiation conversion by the phosphor takes place for the predominant fraction of the reflected short-wave radiation. Thus, the absorption of the blue radiation by the patina results in a reduced fraction of the phosphor-converted photons, which can be manifested by the spectra shown in Fig. 4. Proportionally, the percentage of the total emitted blue photons from the device is reduced to a lower extent, especially since these photons are predominantly emitted directly from the chip without additional reflection processes. The ratio of the emitted spectral components is shown schematically in Fig. 11.

After a mono-atomic layer has formed on the silver reflector, it can be assumed that oxidation proceeds more slowly, especially since deeper silver atoms are protected from chemical reactions by the patina [25]. As a result, optical degradation and the associated color shift will progress more slowly, which is consistent with the results shown in Figs. 3 and 5.

The origins of oxidation-promoting chemicals diffusing into the package are manifold. As the modules were stressed in a laboratory atmosphere ($T_a = 25$ °C, RH = 30%), it is likely that extrinsic corrosion factors had a decisive impact on the oxidation of the silver mirror. These include the outgassing of drivers, cables, or other materials in the direct environment of the devices. Based on the temperature dependence shown in Fig. 10, it can be concluded that the oxidation of the silver reflector is accelerated with increasing temperature. Generally, different processes have to be considered, whose temperature dependence could affect the degradation behavior of the devices.

1) The cables that were used to contact the modules are located partially on the temperature-controlled heat

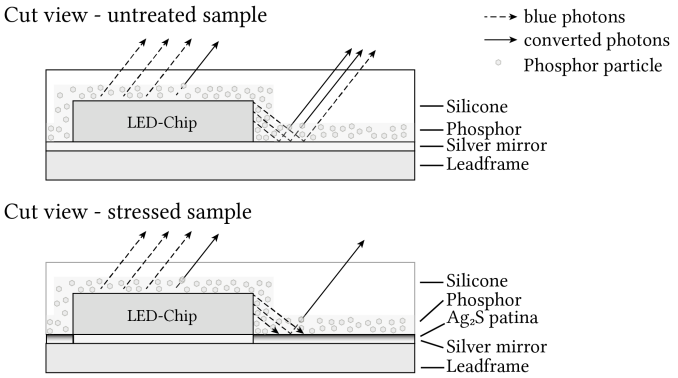

Fig. 11. Schematic cut view of the treated and untreated samples. A tarnished silver mirror reduces the reflection of blue photons, resulting in a significant lower emission of the phosphor-converted photons and thus a strong color shift.

sinks, and thus a temperature-dependent outgassing of sulfur species can be expected. According to Sakai et . [28], the temperature dependency could be described using an Arrhenius equation. The outgassed sulfur species is available for chemical reactions.

2) The permeability of silicone for gases increases with temperature. Analogous to the previously described outgassing processes, the permeability of the material indicates an Arrhenius behavior [28], [29].
3) The oxidation process described in (1)–(3) exhibits an Arrhenius relationship, which is why tarnishing accelerates with increasing temperature [27].
4) Convection processes above the differently tempered heat sinks provide a temperature-dependent transport of sulfur species to the surface of the LED modules [30].

Taking into account the used cooling system and the associated air circulation, a heat-induced convection above the module does not occur. In addition, the forced air circulation makes an increase in cable outgassed sulfur in the direct environment of the module unlikely. The argumentation against a temperature-induced acceleration by 1) and 4) can be manifested by the fact that the outgassed sulfur depends significantly on the mass of tempered cable [28]. Considering the experimental setup, the exposed cable mass varies randomly between the different heat sinks and thus the amount of outgassed sulfur. Furthermore, the modules with different temperatures are located in close distance to each other and cable outgassing would affect multiple modules operated at different temperature conditions. Therefore, it is appropriate to assume a homogeneous concentration of sulfur species within the entire laboratory.

According to Sakai et al. [28], the sulfur species concentration on the silver surface is critical for an oxidation process. Increased silver mirror temperatures could only accelerate the oxidation rates if there are enough reactants available at the mirrors' surface. Consequently, the Arrhenius behavior shown in Fig. 10 is primarily affected by the temperature-dependent permeability of the silicone encapsulant and the resulting concentration of reactants at the silver surface. Sakai et al. [28] determined the activation energy for sulfur atoms diffusing through rubber with $E_a = 63$ kJmol, which is close to the derived value from Fig. 10 with $E_a = 41.5$ kJmol. The Arrhenius behavior and the correlation shown in Fig. 7 allow to infer that no additional aging mechanisms contribute to the optical degradation in the range of junction temperatures between 61 °C and 126 °C. Therefore, the package design seems to be too sensitive to extrinsic corrosions effects, especially since optical degradation occurs in a common laboratory atmosphere with junction temperatures within the manufacturer specification.

V. Conclusion

In this article, the degradation dynamics of high-power LED modules and the underlying aging mechanisms were analyzed. The reduction in optical power and the associated color shift is largely due to an aging mechanism in the LED package. Specifically, the oxidation of the silver reflector used significantly affects the spectral characteristics of the devices. The oxidation process is affected by the conditions prevailing in the device and can be accelerated with increasing temperature and higher concentrations of chemicals in the environment. The activation energy of the process can be quantified with 0.43 eV. Consequently, the results indicate a very sensitive package design that could possibly be optimized by protective layers, more impermeable silicone or a different reflector material.

Acknowledgment

The work reported in this article reflects the author's view and that the ECSEL Joint Undertaking (JU) is not responsible for any use that may be made of the information it contains.

References

[1] V. Haerle et al., "High brightness leds for general lighting applications using the new thingan-technology," *Phys. Status Solidi A*, vol. 201, no. 12, pp. 2736–2739, 2004, doi: 10.1002/pssa.200405119.
[2] M. Wendt and J.-W. Andriesse, "Leds in real lighting applications: From niche markets to general lighting," in *Proc. IEEE Ind. Appl. Conf. 41st IAS Annu. Meeting*, vol. 5, Oct. 2006, pp. 2601–2603, doi: 10.1109/IAS.2006.256905.
[3] C. C. Lin, Y. S. Zheng, H. Y. Chen, C. H. Ruan, G. W. Xiao, and R. S. Liu, "Improving optical properties of white LED fabricated by a blue LED chip with yellow/red phosphors," *J. Electrochem. Soc.*, vol. 157, no. 9, p. H900, 2010, doi: 10.1149/1.3465654.
[4] P. Kailin, R. Guotao, L. Peng, and H. Peng, "Thermal analysis of multi-chip module high power LED packaging," in *Proc. 12th Int. Conf. Electron. Packag. Technol. High Density Packag.*, Aug. 2011, pp. 1–4, doi: 10.1109/icept.2011.6067025.
[5] E. Y. Gatapova, G. Sahu, S. Khandekar, and R. Hu, "Thermal management of high-power LED module with single-phase liquid jet array," *Appl. Thermal Eng.*, vol. 184, Feb. 2021, Art. no. 116270, doi: 10.1016/j.applthermaleng.2020.116270.
[6] B. Zandi, A. Eissfeldt, A. Herzog, and T. Q. Khanh, "Melanopic limits of metamer spectral optimisation in multi-channel smart lighting systems," *Energies*, vol. 14, no. 3, P. 527, 2021, doi: 10.3390/en14030527.
[7] B. Zandi, O. Stefani, A. Herzog, L. J. M. Schlangen, Q. V. Trinh, and T. Q. Khanh, "Optimising metameric spectra for integrative lighting to modulate the circadian system without affecting visual appearance," *Sci. Rep.*, vol. 11, no. 1, pp. 1–14, Dec. 2021, doi: 10.1038/s41598-021-02136-y.
[8] J. Hu, L. Yang, and M. W. Shin, "Electrical, optical and thermal degradation of high power GaN/InGaN light-emitting diodes," *J. Phys. D, Appl. Phys.*, vol. 41, no. 3, Feb. 2008, Art. no. 035107, doi: 10.1088/0022-3727/41/3/035107.

[9] M. Wagner, A. Herzog, H. Ganev, and T. Q. Khanh, "LED aging acceleration—An analysis from measuring and aging data of 14,000 hours led degradation," in *Proc. 12th China Int. Forum Solid State Lighting (SSLCHINA)*, 2015, pp. 75–78, doi: 10.1109/SSLCHINA.2015.7360693.

[10] D. Raul and K. Ghosh, "Performance of chip-on-board and surface-mounted high-power LED luminaires at different relative humidities and temperatures," *Lighting Res. Technol.*, vol. 51, no. 8, pp. 1249–1262, Dec. 2019, doi: 10.1177/1477153518819040.

[11] E. Juntunen, O. Tapaninen, A. Sitomaniemi, and V. Heikkinen, "Effect of phosphor encapsulant on the thermal resistance of a high-power COB LED module," *IEEE Compon., Packag., Manuf. Technol.*, vol. 3, no. 7, pp. 1148–1154, Jul. 2013, doi: 10.1109/TCPMT.2013.2260796.

[12] *Projecting Long Term Lumen Maintenance of LED Light Sources*, Illuminating Engineering Society, Standard IES TM-21-19, 2019.

[13] *CIE 015:2018 Colorimetry*, 4th Ed., International Commission on Illumination (CIE), Vienna, Austria, Oct. 2018, doi: 10.25039/TR.015.2018.

[14] D. L. MacAdam, "Visual sensitivities to color differences in daylight," *J. Opt. Soc. Amer.*, vol. 32, no. 5, pp. 247–274, 1942, doi: 10.1364/JOSA.32.000247.

[15] *ANSI/IES TM-35-19+E1, Technical Memorandum: Projecting Long-Term Chromaticity Coordinate Shift of Led Packages, Arrays and Modules*, Illum. Eng. Soc., New York, NY, USA, 2019.

[16] S. Benkner, S. Babilon, A. Herzog, and T. Q. Khanh, "Combined methodology for accurate evaluation of distance and direction of chromaticity shifts in LED reliability tests," *IEEE Trans. Device Mater. Rel.*, vol. 21, no. 4, pp. 500–507, Dec. 2021, doi: 10.1109/TDMR.2021.3109853.

[17] Y. Ohno and P. Blattner, "CIE: Chromaticity difference specification for light sources," CIE Central Bur., Vienna, Austria, Tech. Note CIE TN 001:2014, 2014.

[18] M. Buffolo, C. De Santi, M. Meneghini, D. Rigon, G. Meneghesso, and E. Zanoni, "Long-term degradation mechanisms of mid-power LEDs for lighting applications," *Microelectron. Rel.*, vol. 55, nos. 9–10, pp. 1754–1758, 2015, doi: 10.1016/j.microrel.2015.06.098.

[19] E. Jung, M. S. Kim, and H. Kim, "Analysis of contributing factors for determining the reliability characteristics of GaN-based white light-emitting diodes with dual degradation kinetics," *IEEE Trans. Electron Devices*, vol. 60, no. 1, pp. 186–191, Jan. 2013, doi: 10.1109/TED.2012.2226039.

[20] M. Meneghini, M. D. Lago, N. Trivellin, G. Meneghesso, and E. Zanoni, "Thermally activated degradation of remote phosphors for application in LED lighting," *IEEE Trans. Device Mater. Rel.*, vol. 13, no. 1, pp. 316–318, Mar. 2013, doi: 10.1109/TDMR.2012.2214780.

[21] P. Appaiah, N. Narendran, I. U. Perera, Y. Zhu, and Y.-W. Liu, "Effect of thermal stress and short-wavelength visible radiation on phosphor-embedded LED encapsulant degradation," *Opt. Mater.*, vol. 46, pp. 6–11, Aug. 2015, doi: 10.1016/j.optmat.2015.03.030.

[22] J. L. Davis, J. Young, and M. Royer, "CALiPER report 20.5: Chromaticity shift modes of LED PAR38 lamps operated in steady-state conditions," EERE Publication Product Library, Washington, DC, USA, 2016.

[23] G. Mura, G. Cassanelli, F. Fantini, and M. Vanzi, "Sulfur-contamination of high power white LED," *Microelectron. Rel.*, vol. 48, nos. 8–9, pp. 1208–1211, 2008, doi: 10.1016/j.microrel.2008.07.005.

[24] J. Farmer et al., "Atmospheric tarnishing of silver-plated laser mirrors," Lawrence Livermore Nat. Lab., Livermore, CA, USA, Tech. Rep. UCRL-ID-128599, 1997, doi: 10.2172/574529.

[25] W. D. Van Driel, X. Fan, and G. Q. Zhang, *Solid State Lighting Reliability Part 2*. Cham, Switzerland: Springer, 2017, pp. 527–547, doi: 10.1007/978-3-319-58175-0.

[26] A. Herrmann et al., "Understanding the transport phenomena leading to tarnishing of the reflecting silver layer causing reduced light output of LEDs," in *Proc. 18th Int. Conf. Thermal, Mech. Multi-Phys. Simul. Exp. Microelectron. Microsyst. (EuroSimE)*, 2017, pp. 1–6, doi: 10.1109/EuroSimE.2017.7926238.

[27] C. J. Yang, C. H. Liang, and X. Liu, "Tarnishing of silver in environments with sulphur contamination," *Anti-Corrosion Methods Mater.*, vol. 54, no. 1, pp. 21–26, Jan. 2007, doi: 10.1108/00035590710717357.

[28] J. Sakai, M. Omoda, and Y. Ishikawa, "Corrosion of silver by outgassing from rubber," *Corrosion Sci. Technol.*, vol. 7, no. 2, pp. 130–133, 2008, doi: 10.1108/00035590710717357.

[29] D. R. Askeland, *Atom Movement Materials*. Boston, MA, USA: Springer, 1996, pp. 111–137, doi: 10.1007/978-1-4899-2895-5_5.

[30] K. Inaba, Y. Ishikawa, and J. Sakai, "Effect of silver surface temperature on sulfide formation behavior in sulfur vapor at constant temperature," *Corrosion Eng.*, vol. 64, no. 5, p. 148, 2015, doi: 10.3323/jcorr.64.188.